A study of new methods for the simultaneous measurement of diffusion and pore structure in catalyst supports
by Mark Clayton Drake

A thesis submitted in partial fulfillment of the requirements for the degree of Master of Science in Chemical Engineering
Montana State University

Abstract:
Two experimental methods were developed for the simultaneous measurement of both pore structure (i.e., surface area and pore-size distribution) and transport parameters in catalyst supports. One method employed a constant pressure (flow) system, and the other used a variable pressure (batch) system. For the batch method, 2,2-dimethylpropane at 273 K was employed using a “model” spherical support, and carbon dioxide at 303 K was used for the flow system using a commercial cylindrical support.

In the batch method, a step change of adsorbing gas was introduced into the diffusion cell by changing the total pressure of the gas. A finite time was required for equilibrium to occur. By modeling this rate of approach to equilibrium, diffusion coefficients in the support were determined. By measuring the diffusivity over a range of relative pressures, the mode of diffusion was determined (i.e., bulk, Knudsen, or surface). After the mode of diffusion was determined, tortuosity factors were calculated From equilibrium measurements, the surface areas were calculated using the Bruhauer, Emmett, and Teller (BET) equation. Since large quantities of data were generated in this experiment, two techniques were used to match the experimental diffusion data to a “unipore” model. The first technique was the initial slope method, which used experimental data with a normalized weight gain less than 0.5. The second method used moment analysis to match the experimental data over the entire time domain. To determine if the “unipore” model was valid, the value of the effective diffusivity which was calculated from the initial slope method should match that calculated from moment analysis.

In the constant pressure flow process, inert helium was initially introduced into the diffusion cell. A step change in adsorbing gas was accomplished by changing the volume percent carbon dioxide while keeping the total pressure constant with the inert gas. Uptake curves were developed at each step change in adsorbing gas concentration. By modeling this rate of approach to equilibrium, diffusion coefficients in the support may be determined. Three models were attempted to describe the uptake curves that were obtained. The results of the models were inconclusive. Because of the inconclusive results, effective diffusivities could not be determined.

A STUDY OF NEW METHODS FOR THE SIMULTANEOUS MEASUREMENT OF DIFFUSION AND PORE STRUCTURE IN CATALYST SUPPORTS

by

Mark Clayton Drake

A thesis submitted in partial fulfillment
of the requirements for the degree

of

Master of Science

in

Chemical Engineering

MONTANA STATE UNIVERSITY
Bozeman, Montana

August 1984

APPROVAL

of a thesis submitted by

Mark Clayton Drake

This thesis has been read by each member of the thesis committee and has been found to be satisfactory regarding content, English usage, format, citation, bibliographic style, and consistency, and is ready for submission to the College of Graduate Studies.

8/2/84
Date

Chairperson, Graduate Committee

Approved for the Major Department

Aug 2, 1984
Date

John T. Sears
Head, Major Department

Approved for the College of Graduate Studies

8-6-84
Date

Graduate Dean

STATEMENT OF PERMISSION TO USE

In presenting this thesis in partial fulfillment of the requirements for a master's degree at Montana State University, I agree that the Library shall make it available to borrowers under rules of the Library. Brief quotations from this thesis are allowable without special permission, provided that accurate acknowledgment of source is made.

Permission for extensive quotation from or reproduction of this thesis may be granted by my major professor, or in his absence, by the Dean of Libraries when, in the opinion of either, the proposed use of the material is for scholarly purposes. Any copying or use of the material in this thesis for financial gain shall not be allowed without my permission.

Signature Mark C. Quade

Date 7-27-84

ACKNOWLEDGMENTS

The author wishes to thank the faculty and staff of the Chemical Engineering Department at Montana State University for their guidance and assistance.

Special thanks to Dr. Douglas M. Smith for his advice and support throughout the course of this research and thesis preparation.

The author also wishes to thank Dr. Frank P. McCandless and Dr. Robert L. Nickelson for the use of their equipment.

Thanks are also extended to David G. Huizenga for the use of the catalysis supports that he developed.

TABLE OF CONTENTS

TABLE OF CONTENTS—Continued

TABLE OF CONTENTS—Continued

LIST OF TABLES

LIST OF FIGURES

Figures Page

NOMENCLATURE

A_m	The area occupied per molecule of adsorbate in the complete monolayer
C	Net heat of adsorption
C_o	Initial concentration
C	Concentration
C_2	Concentration into upper chamber in flow method
d_s	Diameter of unimodal spheres
D	Diffusivity
D_e	Effective diffusivity
D_K	Knudsen diffusivity
f	Fraction of molecules which stick to pore wall
F_1	Flow into diffusion cell in flow method
F_2	Flow into upper chamber in flow method
G	Gibbs free energy
h	Linear isotherm coefficient
ierfc	Integral of the complementary error function
I_o	Modified bessel function of the first kind, zero order
I_1	Modified bessel function of the first kind, order one
J_o	Bessel function of the first kind, zero order
J_1	Bessel function of the first kind, order one
$\overline{K}$	Constant determined by the shape of the pore size distribution curve
L	Length of pore
M	Molecular weight of adsorbate

M_t	Total amount of diffusing substance at time t
M_∞	Total amount of diffusing substance at equilibrium
n	0, 1, 2 for slab, cylinder, and sphere
N	6.023×10^{23} molecules/g-mol
P	Pressure
P_0	Saturation pressure
r	Spatial coordinate
$\bar{r}$	Mean pore radius
r_k	Kelvin radius
rp	Actual pore radius
R	Gas law constant
S	Surface area
t	Depth of the adsorbed film
T	Temperature
V	Concentration of sorbate adsorbed on the surface of the porous media
V_1	Volume of diffusion cell in flow method
V_2	Volume of upper chamber in flow method
$\bar{V}$	Molar volume
V_p	Pore volume
W	Weight of adsorbate adsorbed at equilibrium
W_m	Weight of adsorbate at monolayer capacity
α_n	Roots of $J_0(R\alpha_n)$
β	Gas flow rate divided by the diffusion cell volume
γ	Surface tension
δ	Pellet tortuosity factor

ϵ	Void fraction
μ_1	First absolute moment
ρ_p	Particle density
τ	Thickness of one layer
ϕ	Angle of contact between the liquid and the wall of the capillary

ABSTRACT

Two experimental methods were developed for the simultaneous measurement of both pore structure (i.e., surface area and pore-size distribution) and transport parameters in catalyst supports. One method employed a constant pressure (flow) system, and the other used a variable pressure (batch) system. For the batch method, 2,2-dimethylpropane at 273 K was employed using a "model" spherical support, and carbon dioxide at 303 K was used for the flow system using a commercial cylindrical support.

In the batch method, a step change of adsorbing gas was introduced into the diffusion cell by changing the total pressure of the gas. A finite time was required for equilibrium to occur. By modeling this rate of approach to equilibrium, diffusion coefficients in the support were determined. By measuring the diffusivity over a range of relative pressures, the mode of diffusion was determined (i.e., bulk, Knudsen, or surface). After the mode of diffusion was determined, tortuosity factors were calculated. From equilibrium measurements, the surface areas were calculated using the Brunauer, Emmett, and Teller (BET) equation. Since large quantities of data were generated in this experiment, two techniques were used to match the experimental diffusion data to a "unipore" model. The first technique was the initial slope method, which used experimental data with a normalized weight gain less than 0.5. The second method used moment analysis to match the experimental data over the entire time domain. To determine if the "unipore" model was valid, the value of the effective diffusivity which was calculated from the initial slope method should match that calculated from moment analysis.

In the constant pressure flow process, inert helium was initially introduced into the diffusion cell. A step change in adsorbing gas was accomplished by changing the volume percent carbon dioxide while keeping the total pressure constant with the inert gas. Uptake curves were developed at each step change in adsorbing gas concentration. By modeling this rate of approach to equilibrium, diffusion coefficients in the support may be determined. Three models were attempted to describe the uptake curves that were obtained. The results of the models were inconclusive. Because of the inconclusive results, effective diffusivities could not be determined.

INTRODUCTION

Due to the insecurity of petroleum supplies in the Middle East and shortages in world-wide oil reserves, increased attention has been directed toward new sources of energy. The most promising are heavy crude, shale oil, and coal liquids. Due to the large size of these molecules, they provide difficulties as feedstocks for the petroleum refining industry. Since many of the reactions in refining are catalytic (i.e., cracking, reforming, HDS, and HDN), diffusional resistance in the catalyst support pore structure may be significant. This mass transfer resistance can lead to a reduction in the observed activity of the catalyst.

Catalyst supports are normally chosen to be inert with respect to the reacting system, structurally stable at relatively high temperatures and are available in a variety of forms with surface areas ranging from 1 m^2/g to 1300 m^2/g [1]. Typical porosities for catalyst supports range from 10 to 60% with an average pore radius from 1 to 100 nm [1].

One of the most common supports is silica gel, either in the form of granules or powder. Alumina or a composite of silica and alumina are also widely used. Diatomaceous earth, a naturally occurring form of silica having a surface area in the neighborhood of 50 m^2/g, may be utilized as a powdered carrier. Porous carbon is thermally stable to temperatures of 1273 K or more under inert conditions, and certain forms have the highest known surface areas of any material, up to about 1300 m^2/g. These "activated" carbons are commonly used as catalyst carriers for organic reactions [2].

Two methods are commonly used to calculate the total surface area for catalyst supports. For microporosity or pores less than 2 nm, Dubinin-Polyanyi [3,4] potential theory is employed. For pores in the transition range, with diameters between 2 nm and 20 nm, and macropores with diameters above 20 nm the Brunauer, Emmett, and Teller (BET) [5]

theory is used to determine the total surface area. Due to the fact that this research deals with catalyst supports with a mean pore diameter greater than 2 nm, only the BET theory will be considered. This limitation is a result of the large macromolecules used in the refining industry which can approach the size of a 2 nm pore.

Adsorption studies leading to measurements of pore size and pore size distributions employ the Kelvin equation [6]. This relates the equilibrium vapor pressure of a curved surface, such as that of a liquid in a capillary or pore, to the equilibrium pressure of the same liquid on a plane surface.

From equilibrium weight gain measurements of adsorbents as a function of total pressure, adsorption isotherms are developed. Surface area, total pore volume, and pore size distribution can be determined from the methods discussed earlier.

BET Surface Area

To determine surface area by gas adsorption, one needs to calculate the quantity of adsorbate that is equal to a molecular monolayer on the solid surface. Multiplying this quantity by the cross-sectional area occupied by a single adsorbed molecule yields the surface area of the catalyst. This is calculated using the BET equation in which the amount of gas adsorbed on the solid at constant temperature is measured as a function of total pressure of adsorbate gas. The BET equation is [6]:

$$\frac{1}{W[(P_0/P) - 1]} = \frac{1}{W_m C} + \frac{C-1}{W_m C}\frac{P}{P_0} \qquad (1)$$

where

W = weight of adsorbate adsorbed at equilibrium

P = pressure at equilibrium

P_0 = saturation pressure of the adsorbate

W_m = weight of adsorbate at monolayer capacity

C = net heat of adsorption, called the BET **C** value.

A plot of $1/W(P_0/P - 1)$ versus P/P_0 will yield a straight line. Values of W_m and **C** can be calculated from the slope $[(C-1)/W_mC]$ and the intercept $[1/W_mC]$.

The applicability of the BET theory is limited to the range of relative pressures between 0.05 and 0.35, representing the linear BET range. This can be attributed to the assumption that all adsorption sites are energetically equal. The model ignores the influence of lateral adsorbate interactions. Brunauer [7] answers these criticisms by pointing out that lateral interaction between adsorbate molecules increases as the surface becomes more completely covered. The adsorption potential, however, decreases with increasing adsorption up to monolayer coverage. By assuming an energetically heterogeneous surface, the high-energy sites will be occupied at lower relative pressures and occupancy of the lower-energy sites will occur near the completion of the monolayer. These two trends can lead to a nearly constant overall adsorption energy up to completion of the monolayer, which is an implicit assumption of the BET theory. Finally the second and higher layers of molecules have energies assumed to be equal to the heat of liquefaction. For the most reliable measurements the molecules of the gas chosen should be small, approximately spherical, and inert so no chemisorption takes place.

Having determined the monolayer capacity, the specific surface area, $S(m^2/g)$, is calculated by [8]:

$$S = \frac{W_m}{M} N \cdot A_m \times 10^{-20} \qquad (2)$$

W_m = monolayer capacity of adsorbate

M = molecular weight of adsorbate

N = Avogadro's constant

A_m = the area occupied per molecule of adsorbate in the complete monolayer.

In order to use Equation 2, it is necessary to know the value of the cross-sectional area A_m. The value of this quantity is difficult to calculate because of our lack of knowledge as to the exact packing of the adsorbed molecules in a complete monolayer.

Emmett and Brunauer [9] proposed that A_m be calculated from the density of the adsorbate in the liquid form. They assumed that the arrangement of the molecules on the surface was similar to that on a plane surface placed within the bulk of the liquid. For twelve nearest neighbors in the bulk liquid and six on the plane we then have the equation [8]:

$$A_m = 1.091 \left(\frac{M}{\rho N}\right) \times 10^{16} \tag{3}$$

This yields values of 0.162 nm^2, 0.195 nm^2, and 0.625 nm^2 for nitrogen [9] (77 K), CO_2 [11] (273 K), and 2,2-dimethyl propane [10] (273 K), respectively.

Pore Size Distribution

Two methods are commonly used to determine the pore size distribution. One is Mercury Porosimetry, using the Washburn equation and the second is application of the Kelvin equation to adsorption-desorption isotherms.

The Kelvin equation [6], which had been established originally by Thompson [12] (later by Lord Kelvin), relates the vapor pressure of a curved surface, such as that of a liquid in a capillary or pore, to the equilibrium pressure of the same liquid on a plane surface. The increase in the amount of vapor adsorbed onto a catalyst support, as a result of an incremental increase in vapor pressure at constant temperature, represents the filling of capillaries the size of which is given by the Kelvin equation. The size of the largest pore that can be measured is limited by the rapid change of meniscus radius with pressure as the

relative pressure, P/P_0, nears unity. This is generally taken as about 30 nm in diameter, corresponding to a relative pressure of 0.93 [2]. The smallest pore sizes that can be determined by this method are about 1.5-2 nm in diameter. This is because the molecules equipotential lines interact with each other in these small pores and the Kelvin equation no longer applies.

A somewhat different relationship between the amount of vapor sorbed and pressure is usually obtained experimentally upon decreasing rather than increasing the pressure [2]. This difference is known as a hysteresis effect. Figure 1 depicts hysteresis which is typical of porous adsorbents on type IV isotherms [8]. De Boer [13] describes this as a type A hysteresis which is due mainly to cylindrical pores open at both ends. The five types of de Boer's hysteresis will be described later. The line BCD indicates the path followed along the adsorption isotherm, whereas line DFB demonstrates the path followed along the desorption isotherm. The presence of the hysteresis loop introduces considerable complications because there are two relative pressures that correspond to a quantity adsorbed. Figure 1 shows that the weight W adsorbed is at a lower relative pressure on the desorption curve than on the adsorption isotherm. The molar free energy change from the condensation of the vapor into the pore during adsorption is determined by:

$$\Delta G_{ads} = RT(\ln P_{ads} - \ln P_0) \tag{4}$$

For the same quantity on the desorption isotherm, the free energy change is

$$\Delta G_{des} = RT(\ln P_{des} - \ln P_0) \tag{5}$$

Since $P_{des} < P_{ads}$, it follows that $\Delta G_{des} < \Delta G_{ads}$. Therefore, the desorption isotherm is preferred because it is the more stable condition [8].

Several theories have been postulated to describe hysteresis during adsorption and desorption. Zsigmondy [14] attributed hysteresis to a difference in the contact angle during adsorption and desorption. McBain [15] accounted for the hysteresis by assuming the

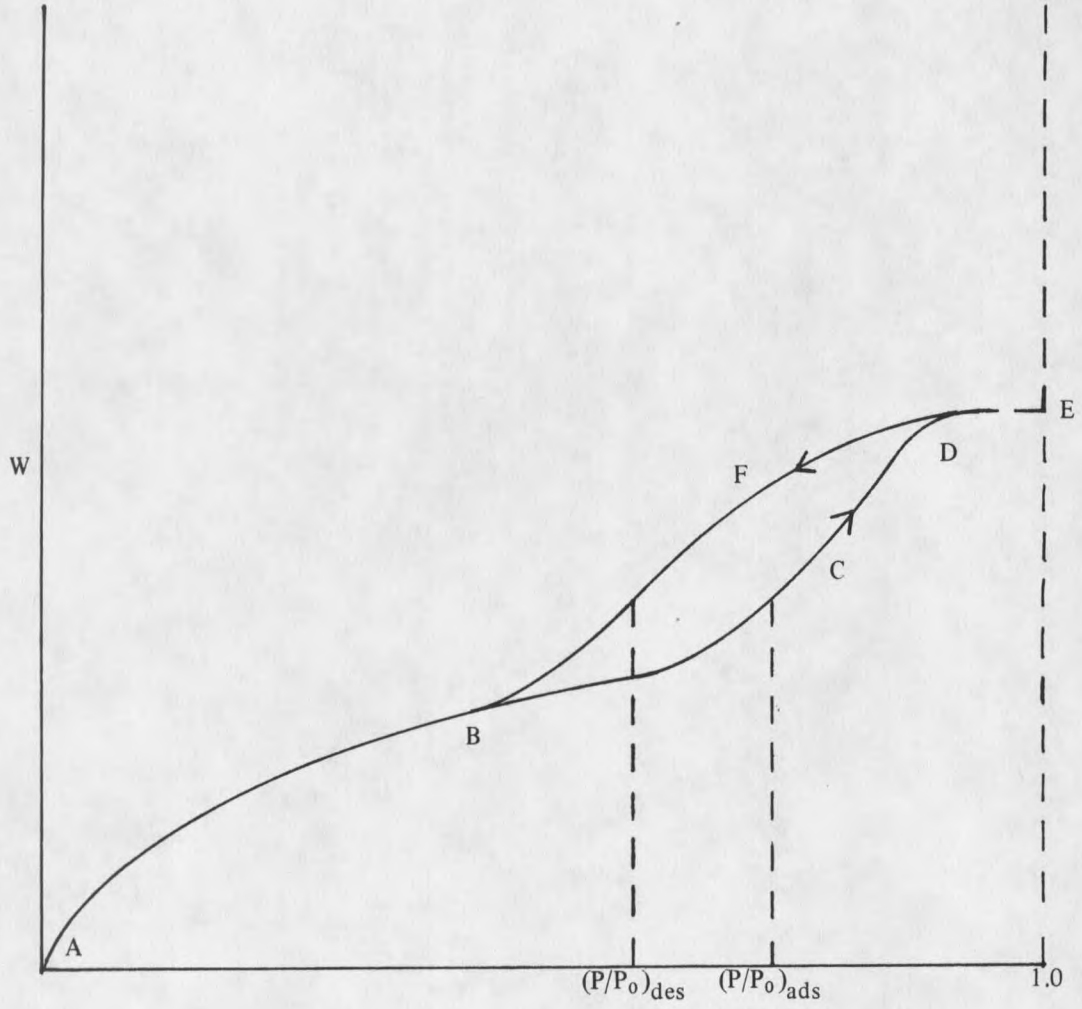

Figure 1. Typical type IV adsorption and desorption isotherms showing hysteresis.

pores contained a narrow opening and a wide body, the so-called "bottleneck" shape. Cohan [16] assumed that condensation occurs by filling the pore from the wall inward. For a cylindrical pore, this would give a cylindrical shaped meniscus whereas evaporation occurs from a hemispherical meniscus once the pore is filled. Foster [17] explained hysteresis by considering the pores to fill by adsorption on the walls while emptying by evaporation from a spherical meniscus. These theories each describe reasons for the occurrence of hysteresis, but no one theory appears to provide a complete explanation.

De Boer [13] has identified five types of hysteresis loops which he has correlated with various pore shapes. Figure 2 shows the five types of hysteresis. Type A is mostly due to cylindrical pores open at both ends. Type B is associated with slit-shaped pores or a space between parallel plates. Type C is produced by a mixture of tapered or wedge-shaped pores with open ends. Type D curves are also produced by tapered or wedge-shaped pores with narrow necks at one or both ends. Type E results from McBain's "bottleneck" pores.

To measure pore size and pore size distributions the Kelvin equation is applied [6,8]

$$\ln\left(\frac{P}{P_0}\right) = -\frac{2\bar{V}\gamma}{rRT}\cos\phi \qquad (6)$$

where

P_0 = saturation vapor pressure

γ = surface tension

$\bar{V}$ = molar volume

ϕ = the angle of contact between the liquid and the walls of the capillary

r = radius of the pore.

Usually knowledge of the pore geometry is not known. Because of this, the assumption of cylindrical pores is made. It is also necessary to assign a value to the angle of contact between the liquid and the pore walls. This quantity is extremely difficult to determine directly in the case of porous solids. The usual assumption is to set the contact angle equal to zero.

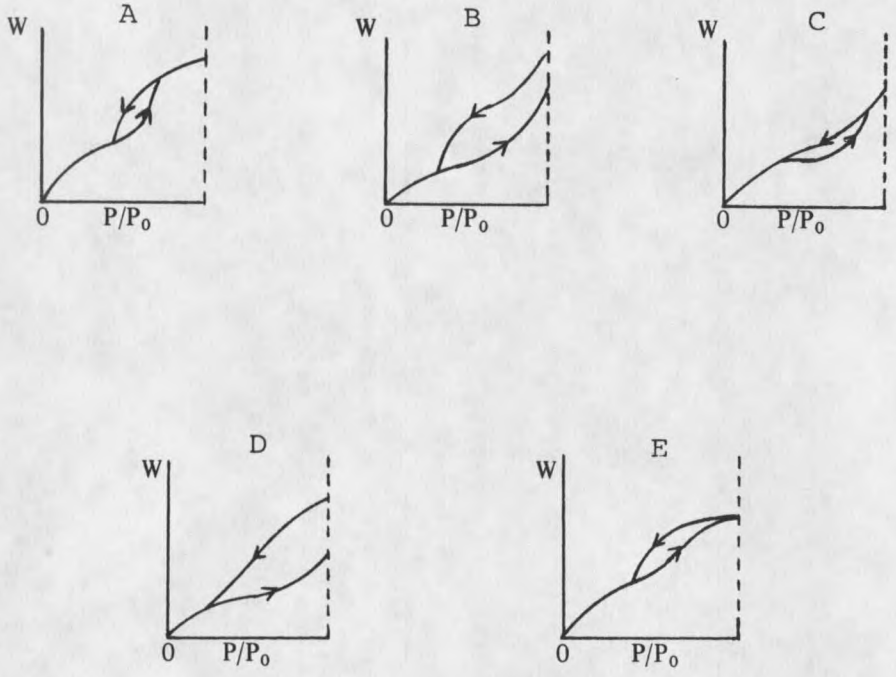

Figure 2. The five isotherms classifications according to De Boer [13].

From Equation 6, the Kelvin radius, r_k, can be calculated. This is not the true radius because adsorption has occurred on the pore wall, prior to condensation, leaving a center core of radius r_k.

With the depth of the adsorbed film being t, then the actual pore radius, r_p, is

$$r_p = r_k + t \tag{7}$$

It is now necessary to calculate t.

Using the assumption that the adsorbed film depth in a pore is the same as on a plane surface for any value of relative pressure, one may write

$$t = \left(\frac{W_a}{W_m}\right) \cdot \tau \tag{8}$$

where W_a and W_m are respectively, the quantity adsorbed at a particular relative pressure and the weight corresponding to the BET monolayer. τ is the thickness of one layer. The value of τ can be calculated by considering the area and volume occupied by one mole of liquid adsorbate if it were spread over a surface to the depth of one molecular layer.

$$\tau = \frac{\bar{V}}{S} \tag{9}$$

where $\bar{V}$ is the molar volume and S is the surface area occupied by one mole of the sorbate when a single layer is formed.

Further details for pore size distribution calculations are given in Lowell [8] and Gregg and Sing [6].

Methods for Measuring Transport Parameters

Several methods are available to measure transport parameters. These methods are divided into two categories, either steady-state or transient. Many unit operations in engineering do not operate in the steady-state. Examples include ion-exchange columns, adsorption towers and packed beds. Therefore, transport parameters must be calculated from

transient methods for these systems. It is the intent of this study to provide a means by which to calculate one particular transport parameter, the effective diffusivity. Comparison of effective diffusivities from steady-state and dynamic experiments can, in principle, provide information about pore structure. For example, dead-end pores should not affect diffusion at steady state, but would influence the diffusion coefficient in dynamic experiments.

Steady-State Methods

Two types of experiments are in common use for studying steady-state diffusion in porous solids. The most frequently used method for steady-state operation is the Wicke-Kallenbach [18] diffusion cell, also known as the constant pressure, counter diffusion cell. In this experiment, the ends of the catalyst pellet are exposed to either an adsorbing or a non-adsorbing gas such that no pressure gradients occur across the sample. Diffusion rates are determined from the flow rates and concentrations of the two outlet streams. The "plug flow" experiment, as the name implies, uses a plug of the porous solid of interest through which the desired gas is forced. By measuring the gas flow rate and the pressure drop across the sample, the diffusivity can be calculated.

The constant pressure, counter diffusion experiment offers advantages over the "plug flow" type experiment. These advantages are [19]:

1. By eliminating the total pressure gradient, the computation of effective diffusivities is simplified.
2. By measuring both gas fluxes simultaneously, the time required for the experiment is halved.

Transient Methods

To determine unsteady-state effective diffusivities, three types of experiments are commonly used. The first method employs volumetric measurements. This is accomplished by introducing a step change of an adsorbing gas into the chamber containing the catalyst support. The size of the chamber and the step change concentration in adsorbing gas must be small to insure that the surface concentration remains constant. The pressure change versus time is then measured. From this data and an appropriate model describing the system, transport coefficients can be determined. The advantage for using the volumetric method is that it can be used for light gases (i.e., low molecular weight) which would not produce a large enough weight gain to be used with gravimetric techniques.

The second method uses pulse tracer (chromatographic) experiments for the determination of diffusivities. Various investigations using these techniques are reviewed by Smith [20] and Satterfield [21]. By passing a pulse of tracer gas through either a fixed-bed, ion-exchange column or a single catalyst pellet, transport coefficients may be obtained by relating the shape of the response pulse to a model describing the system.

The third type of experiment employs gravimetric techniques. Generally, two types of gravimetric balances are used in catalyst research, spring extension [22] and the null beam balance [23,24]. The spring balance usually employs a quartz spiral. Weight change is proportional to the spring extension, the measurement being made visually and intermittently with a cathetometer or automatically by a suitable transformer coupled to electronic equipment giving a continuous voltage output. Disadvantages of the spring balance are limited loading capacity for a given sensitivity and displacement of the sample position with a change in weight [25].

The beam balance uses tare weights, and null principle so that the sample remains in a fixed position. Weight changes are then detected by application of a suitable counterforce

to maintain the null position, the counterforce being converted to voltage which is recorded versus time on a computer acquisition system. To determine transport parameters, a step change in adsorbing gas is introduced into the diffusion cell. A finite time is required for equilibrium to occur. From this rate of approach to equilibrium data an appropriate model is then constructed. Transport parameters can be determined from the model.

The advantages of gravimetric measurements are: only a small sample size is needed; measurements can be made at constant or variable pressure; readings are automatic and continuous; and operation can be static or under flow conditions. The disadvantage is that an adsorbing gas is needed.

Research Objectives

The objective of this research project was to examine an experimental procedure for the simultaneous measurement of both pore structure (i.e., surface area and pore-size distribution) and an effective diffusivity in several catalyst supports. Two different experimental adsorption techniques were to be evaluated, one using a constant pressure flow cell and the other utilizing a variable pressure batch cell. Diffusion models describing each system were to be constructed to evaluate effective diffusivities.

DIFFUSION MODELS

To determine the effective diffusivity in porous media, an appropriate physical model describing the system must be developed. The effective diffusivity calculated via appropriate model matching techniques is put into the solution of the model and a sorption curve is then generated. This is then compared with the experimental data. If the curve generated matches the experimental data the diffusion coefficient calculated is appropriate.

Mechanism of Transport into Pores

The diffusion of an adsorbing gas through porous media may occur due to any of three possible mechanisms. A knowledge of the mechanisms of diffusion is required in order to determine the tortuosity factor and to ascertain the effect of pressure and temperature on the transport rate.

The three possible mechanisms are bulk, Knudsen and surface diffusion. When the pore size is much greater than the mean free path of the gas, intramolecular collisions dominate and gas diffusion is purely bulk diffusion. If the pore size is much smaller than the mean free path of the diffusing gas, Knudsen diffusion will predominate the rate of molecular movement. As a result a molecule within the pore structure will, in general, strike a pore wall before it strikes a second molecule. Intramolecular collisions may thus be neglected. The molecule then travels within the pore by a series of "random flights" interrupted by collisions with the pore wall [26]. When the pore size approaches the mean free path, intramolecular and molecule wall interactions are both important. This is called the transition region. In addition to the two gas phase mechanisms, transport of adsorbed gases along the surface may occur. This surface diffusion has been explained as a flow

of the outer layers as a condensed phase. The overall flux of a gas through porous media may be any one or a combination of the three mechanisms stated above.

Adsorption Effects

Two assumptions were made dealing with adsorption effects. The first is that sorption can be described by the linear isotherm

$$V = hC \tag{10}$$

where

V = concentration of the sorbate adsorbed on the surface of the porous media

h = linear isotherm coefficient

C = concentration of sorbate in the gas phase

This is usually valid at low concentrations. The second is that the rate of adsorption is assumed to be much more rapid than the rate of diffusion (i.e., there is physical adsorption only).

"Unipore" Model

Although the theory of diffusion in a single capillary is well developed, the application of this theory to practical problems is quite complex. In order to apply the findings of capillary theory, a physical model of the porous media must be assumed.

The "unipore" or "parallel pore" model as developed by Wheeler [26] has received wide application in studying porous media due to its conceptual and mathematical simplicity. A porous particle is presumed to be a solid with a system of parallel, nonconnecting cylindrical pores of the same size. A shortcoming of the parallel pore model is its failure to account for intersections and deadends. A modification to the "unipore" model is the addition of a tortuosity factor. This factor is a semiempirical constant employed in an attempt to overcome the above mentioned shortcoming [19].

The following assumptions were made in the development of the "unipore" model:

1. Equilibrium between the gas and adsorbed phases.
2. The diffusion coefficient is constant.
3. Diffusion is one dimensional (no edge effects).
4. The particle has zero concentration initially.

These assumptions were made to minimize the number of parameters considered and will result in findings which may be applied to experiments with multiple particles.

The mass balance for either slab, cylindrical or spherical geometries is

$$\frac{D\epsilon}{\delta r^n} \frac{\partial}{\partial r}\left(r^n \frac{\partial C}{\partial r}\right) = \frac{\partial C}{\partial t} + \frac{\rho_p}{\epsilon} \frac{\partial V}{\partial t} \tag{11}$$

where

n = 0, 1, 2 for slab, cylinder, and sphere

D = diffusion coefficient (i.e., bulk, Knudsen, or surface diffusion)

r = spatial variable

C = concentration

t = time

ϵ = porosity of the particle

ρ_p = particle density

δ = tortuosity

The initial and boundary conditions are as follows

$$C(r,0) = 0, \quad C(R,t) = C_o(t), \quad \frac{\partial C}{\partial r}(0,t) = 0 \tag{12}$$

When the sorbed phase is assumed to be in equilibrium with the gas phase, the source/sink term ($\partial V/\partial t$) is obtained by taking the derivative of the sorption-isotherm Equation 10:

$$\frac{\partial V}{\partial t} = h \frac{\partial C}{\partial t} \tag{13}$$

Substituting Equation 13 into Equation 11 gives

$$\frac{D\epsilon}{\delta r^n}\frac{\partial}{\partial r}\left(r^n\frac{\partial C}{\partial r}\right)=\left(1+\frac{h\rho_p}{\epsilon}\right)\frac{\partial C}{\partial t} \tag{14}$$

Defining an effective diffusivity by

$$D_e=\frac{D\epsilon}{\delta\left(1+\frac{h\rho_p}{\epsilon}\right)} \tag{15}$$

and combining Equation 14 with Equation 15, the governing equation for transient uptake in a porous particle is

$$\frac{D_e}{r^n}\frac{\partial}{\partial r}\left(r^n\frac{\partial C}{\partial r}\right)=\frac{\partial C}{\partial t} \tag{16}$$

The fractional uptake as a function of time is

$$\frac{M_t}{M_\infty}=\frac{{}_0\int^R r^n\,C(r,t)dr}{{}_0\int^R r^n\,C(r,\infty)dr} \tag{17}$$

where

M_t = the total amount of diffusing substance at time t

M_∞ = the total amount of diffusion substance at equilibrium

Surface Concentration Constant

This is the case where the initial concentration in the porous media is zero, and the surface concentration is instantaneously changed to C_o.

The initial and boundary conditions are

$$C(r,0)=0,\quad C(R,t)=C_o,\quad \frac{\partial C}{\partial r}(0,t)=0 \tag{18}$$

Solutions for the slab, cylindrical and spherical geometries are now presented.

Slab. The sorption time curve is given by [27]:

$$\frac{M_t}{M_\infty} = 1 - \sum_{n=0}^{\infty} \frac{8}{(2n+1)^2\,\pi^2}\, e^{-D_e(2n+1)^2\,\pi^2\,t/4R^2} \tag{19}$$

where R = one half of the diffusion path length.

Although Equation 19 predicts the quantity of gas adsorbed as a function of time and the effective diffusivity, convergence problems exist at short times and an alternative form should be used. The corresponding solution useful for small times is [28]

$$\frac{M_t}{M_\infty} = 2\left(\frac{D_e t}{R^2}\right)^{1/2} \left\{ \pi^{-1/2} + 2 \sum_{n=1}^{\infty} (-1)^n \operatorname{ierfc}\left(\frac{nR}{\sqrt{(D_e t)}}\right) \right\} \tag{20}$$

Cylinder. The solution for diffusion into a cylinder is given by [27]:

$$\frac{M_t}{M_\infty} = 1 - \sum_{n=1}^{\infty} \frac{4}{R^2\,\alpha_n^2}\, e^{-D_e\,\alpha_n^2\,t/R^2} \tag{21}$$

where

R = radius of the cylinder

α_n = roots of $J_o(R\alpha_n)$

The corresponding solution for small times is [28]

$$\frac{M_t}{M_\infty} = \frac{4}{\pi^{1/2}}\left(\frac{D_e t}{R^2}\right)^{1/2} - \frac{D_e t}{R^2} - \frac{1}{3\pi^{1/2}}\left(\frac{D_e t}{R^2}\right)^{3/2} + \ldots \tag{22}$$

Sphere. The total amount of diffusion substance entering or leaving a sphere is given by [27]:

$$\frac{M_t}{M_\infty} = 1 - \frac{6}{\pi^2} \sum_{n=1}^{\infty} \frac{1}{n^2}\, e^{-D_e n^2 \pi^2 t/R^2} \tag{23}$$

where R = radius of the sphere.

The corresponding solution for small times is [28]:

$$\frac{M_t}{M_\infty} = 6\left(\frac{D_e t}{R^2}\right)^{1/2}\left\{\pi^{-1/2} + 2\sum_{n=1}^{\infty} \text{ierfc}\left(\frac{nR}{\sqrt{(D_e t)}}\right)\right\} - 3\,\frac{D_e t}{R^2} \qquad (24)$$

Curves comparing the three geometries show M_t/M_∞ as a function of $(D_e t/R^2)^{1/2}$ and are presented in Figure 3.

Model Matching Techniques. Two techniques are presented that allow the determination of an effective diffusivity from experimental data. The first is the initial slope method which uses the experimental data at short times. The second method utilizes moment analysis which uses experimental data over the whole time domain.

Initial Slope Method. For M_t/M_∞ less than 0.5, the following approximations are used:

$$\frac{M_t}{M_\infty} = \frac{2(n+1)}{\sqrt{\pi}}\left(\frac{D_e t}{R^2}\right)^{1/2} \qquad (n=0,1,2) \qquad (25)$$

By plotting the fraction adsorbed, M_t/M_∞, versus $\sqrt{\text{time}}$, an effective diffusivity can be calculated from the linear region.

Moment Analysis. Effective diffusivities may also be determined using the experimental data over the entire time domain. This can be ascertained from moment analysis using the first absolute moment. The solution to Equations 16 to 18 is obtained in the Laplace domain, where the moments are given by [24]:

$$m_i = (-1)^i \left.\frac{d^i(\tilde{M}_t/\tilde{M}_\infty)}{ds^i}\right|_{s=0} \qquad (26)$$

and $\tilde{M}_t/\tilde{M}_\infty$ is the Laplace transform of M_t/M_∞. The solution to this problem for the first absolute moment is [22]:

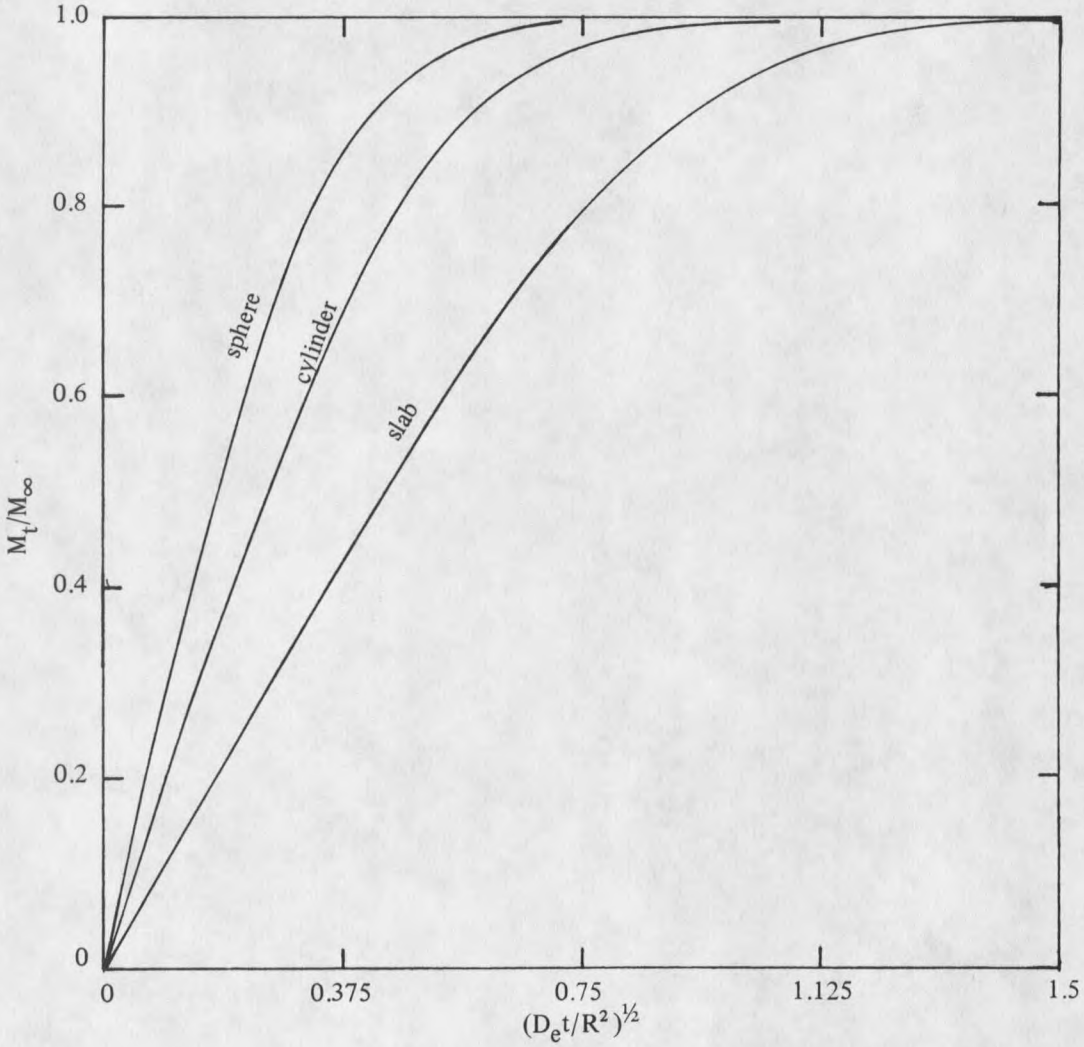

Figure 3. Sorption curves for slab, cylindrical and spherical geometries with surface concentration C_o.

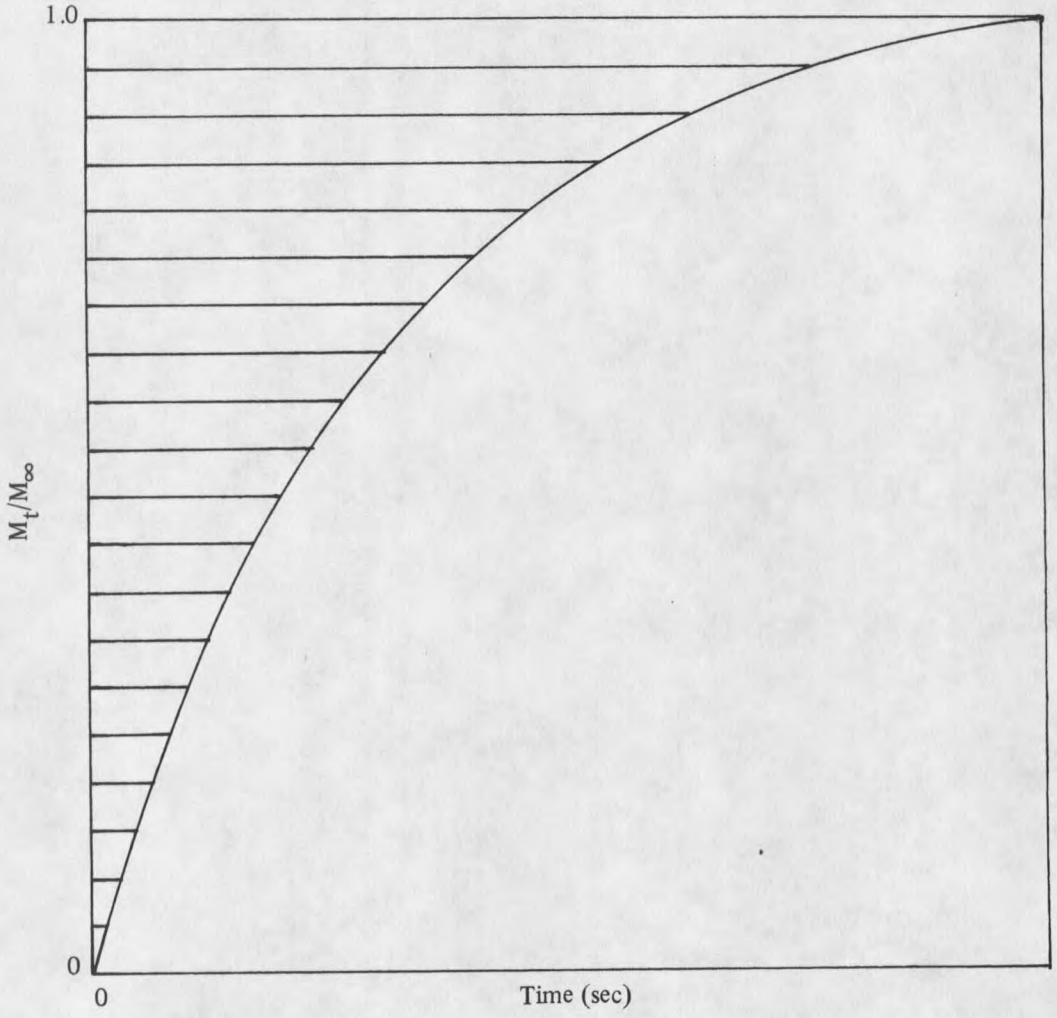

Figure 4. The shaded area represents the first statistical moment.

$$\mu_1 \equiv \frac{m_1}{m_0} = \frac{1}{(n+1)(n+3)} \frac{R^2}{D_e} \qquad (n=0,1,2) \qquad (27)$$

The moments of the experimental (monotonically increasing) curves M_t/M_∞ versus time can be related to the moments of the (monotonically decreasing) complementary curve $(1 - M_t/M_\infty(t))$ versus time, as [24]:

$$m_i = i_0 \int^{\infty} (1 - M_t/M_\infty (t))\, t^{i-1}\, dt \qquad (28)$$

The shaded area in Figure 4 represents the moments calculated from Equation 28. Equating Equations 27 and 28, an analytic expression involving the diffusion coefficient is obtained. Appendix 2 contains an algorithm that will evaluate the first through fourth moments from M_t/M_∞ versus time data.

Comparison of Initial Slope and Moment Analysis. To determine if the "unipore" model is valid for the porous media in question, the value of D_e, which is calculated for short times only should match that calculated from data over the whole time domain. If the effective diffusivities calculated from the two methods do not match, then the "unipore" model is not adequate for this material and another model should be developed.

Variable Surface Concentration

This is the case where the initial concentration in the porous media is initially zero, and the surface approaches an equilibrium concentration C_o exponentially. This can represent a surface concentration which is changed rapidly but not instantaneously, a situation which usually arises when an instantaneous change is attempted in an experiment.

The initial and boundary conditions are:

$$C(r,0) = 0, \quad C(R,t) = C_o(1 - e^{-\beta t}), \quad \frac{\partial C}{\partial r}(0,t) = 0 \qquad (29)$$

where

β = F/V

V = diffusion cell volume

F = volumetric flow rate

Presented are solutions for the slab, cylindrical and spherical geometries for diffusion when each surface approaches an equilibrium concentration, C_o, exponentially.

Slab. The sorption time curve is given by [27]:

$$\frac{M_t}{M_\infty} = 1 - e^{-\beta t}\left(\frac{D_e}{\beta R^2}\right)^{1/2} \tan\left(\frac{D_e}{\beta R^2}\right)^{1/2} - \\ - \frac{8}{\pi^2} \sum_{n=0}^{\infty} \frac{e^{-(2n+1)^2 \pi^2 D_e t/4R^2}}{(2n+1)^2\left[1 - (2n+1)^2\left\{\frac{D_e \pi^2}{4\beta R^2}\right\}\right]} \qquad (30)$$

where R = one half the path length, and β is not equal to $D_e(2n+1)^2\pi^2/4R^2$.

Cylinder. The sorption versus time curve is given by [27]:

$$\frac{M_t}{M_\infty} = 1 - \frac{2J_1\left\{(\beta R^2/D_e)^{1/2}\right\} e^{-\beta t}}{(\beta R^2/D_e)^{1/2} J_0\left\{(\beta R^2/D_e)^{1/2}\right\}} + \frac{4}{R^2} \sum_{n=1}^{\infty} \frac{e^{-D_e \alpha_n^2 t}}{\alpha_n^2\left\{\frac{\alpha_n^2}{(\beta/D_e)} - 1\right\}} \qquad (31)$$

where

R = radius of the cylinder

α_n = roots of $J_0(R\alpha_n)$

Sphere. The sorption-time curve is given by [27]:

$$\frac{M_t}{M_\infty} = 1 - \frac{3D_e}{\beta R^2} e^{-\beta t}\left[1 - \left(\frac{\beta R^2}{D_e}\right)^{1/2} \mathrm{Cot}\left(\frac{\beta R^2}{D_e}\right)^{1/2}\right] +$$

$$+ \frac{6\beta R^2}{\pi^2 D_e} \sum_{n=1}^{\infty} \frac{e^{-D_e n^2 \pi^2 t/R^2}}{n^2(n^2\pi^2 - \beta R^2/D_e)} \qquad (32)$$

where R = radius of the sphere.

Figure 5 compares uptake curves for slab, cylindrical and spherical geometries plotted against $(D_e t/R^2)^{1/2}$ with the parameter $\beta R^2/D_e$ equal to 3. Figure 6 depicts uptake curves for cylindrical geometry with different values of the parameter $\beta R^2/D_e$ plotted against $(D_e t/R^2)^{1/2}$. When $\beta = \infty$, the surface concentration rises instantaneously to C_o and the curve of Figure 6 has the characteristic initial linear portion followed by the approach to the equilibrium value, M_∞. The uptake curves for finite values of $\beta R^2/D_e$, for which the surface concentration rises at a finite rate, all show points of inflexion. At first the rate of uptake increases as sorption proceeds but later decreases as the final equilibrium is approached. Curves of this kind are often referred to as sigmoid sorption curves [20].

Moment Analysis. Since finite values of $\beta R^2/D_e$ give sigmoid sorption curves, the small time portion of the uptake curve is not linear, therefore the initial slope method cannot be used. Effective diffusivities are determined using Equations 26 and 27 to evaluate the first absolute moment.

The solution of Equations 16, 17, and 29 is

$$\mu_1 \equiv \frac{m_1}{m_o} = \frac{1}{\beta} + \frac{1}{(n+1)(n+2)} \frac{R^2}{D_e} \qquad (n=0,1,2) \qquad (33)$$

Derivations for the first absolute moment for all three geometries is given in Appendix 1.

The effective diffusivities are determined using Equation 33 and μ_1 is calculated from the moment algorithm given in Appendix 2.

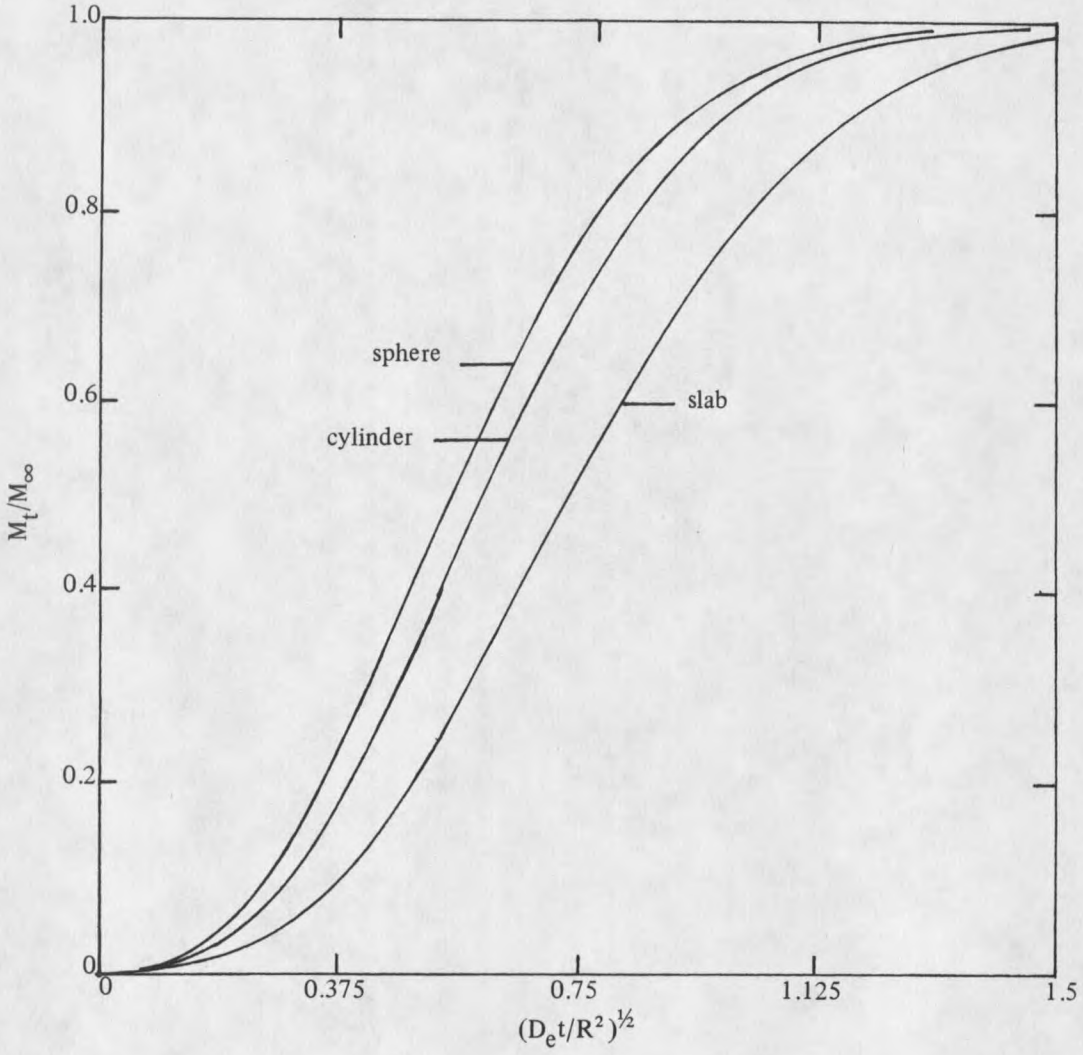

Figure 5. Sorption curves for slab, cylindrical and spherical geometries for surface concentration given by $C_o \left\{ 1 - \exp(-\beta t) \right\}$.